

ELECTROMAGNETIC AND MUONIC STRUCTURE OF SHOWERS INITIATED
BY GAMMA-RAYS AND BY HADRONS

A. M. Hillas
Physics Department, University of Leeds,
Leeds LS2 9JT, UK

ABSTRACT

(a) If photon cascades develop by the usual mechanisms, there should indeed be notable differences between the structure of showers due to photon and hadron primaries, as regards muon densities and lateral distributions of some detector signals.

(b) The muon content of showers from Cygnus X-3, observed at Kiel, cannot be understood in this way. One remedy is to postulate arbitrarily a strong hadronic interaction of photons in the TeV region. This would utterly change the nature of electromagnetic cascades, but surprisingly does not at first sight seem to be in conflict with air shower observations.

1. Two questions concerning gamma-ray initiated showers

(i) Can the structure of extensive air showers ($10^{15} - 10^{16}$ eV) be used to distinguish those that are initiated by primary gamma-rays from the normal proton- or nucleus- initiated showers? This would help in observations of point sources such as Cygnus X-3. The low muon content of gamma showers has been regarded as their most obvious hallmark, with different shower "age" as another possible distinguishing feature. However,

(ii) can one understand the observation by Samorski & Stamm (1) that showers from Cygnus X-3 (whose primaries are undeflected and stable, and hence presumably photons) have about 2/3 of the normal density of penetrating particles (muons of 2 GeV or more) at ~ 10 m from the shower axis?

If the directional particle fluxes being reported from various proton decay experiments are confirmed, they indicate that the radiation from Cygnus X-3 has important interactions that are not yet understood.

2. Calculation of shower development

A 3-dimensional Monte-Carlo simulation is used to follow all particles (electrons, photons, nucleons, pions, muons - but omitting kaons) down to 0.05 MeV, and to determine the signals produced in 5-cm-deep scintillators and 120-cm-deep water Cerenkov detectors (as used at Haverah Park). (The average response of such detectors - covered by a thin wood roof - to the relevant particles and energies was calculated beforehand, but, as a check, the shower particles were followed into a 120-cm-deep lake on reaching the ground, where their Cerenkov emission was noted and the ionization loss in the top layer was also noted to check the scintillator response.)

Assumptions about hadronic interactions of photons: Up to several GeV, $\sigma(\gamma, \text{air nucleus} \rightarrow \text{hadrons}) = 6.4 \sigma(\gamma, \text{deuteron})$. The intermediate states produced in the well-known resonances below 1 GeV were taken to decay isotropically (in c.m.s.) as an approximation, in 2-body stages. However, these resonances are of little importance in EAS: most of the muons resulting (via pion decay) are of such low energy that they stop - and certainly none is above 2 GeV. From 10 GeV to 200 GeV the cross-section is taken to be 1.42 mb, and then to rise rather like p-p cross-sections - i.e. $1.42 (1 + 0.0273u + 0.01u^2)$ mb, where $u = \ln(E/200 \text{ GeV})$. Interacting photons are taken to behave very much like pions.

Assumptions about hadron interactions. Two models of hadronic interactions are used: (a) a radial scaling model (with rising hadron-nucleon cross-sections), based on detailed accelerator data up to 1 TeV, but making the approximation of working with scaling in the laboratory frame of reference (thus underestimating a little the particles below ~ 1 GeV); (b) a modification in which a greater multiplicity of low-x particles is generated (but without a large reduction in the fragmentation-region particles) at collision energies above ~ 1 TeV, and fewer leading pions are produced. These two variants are thought to bracket the true main features of interactions. Roughly speaking, the first model with a large content of very heavy nuclei in the primary beam, or the latter with largely protons, would account for many air shower features.

3. Proton-initiated and gamma-initiated showers

Figure 1 shows the apparent particle densities ρ at various axial distances, in showers produced by normal primaries of 10^{14} , 10^{15} , 10^{16} and 10^{17} eV per nucleon, and by gammas of 10^{15} and 10^{16} eV, all at 15° zenith angle. All are normalized to 10^{16} eV energy, by plotting $r^2\rho/E_{16}$, where $E_{16} = E_{\text{prim}}/10^{16}$ eV. Particle densities recorded by deep water tanks, and

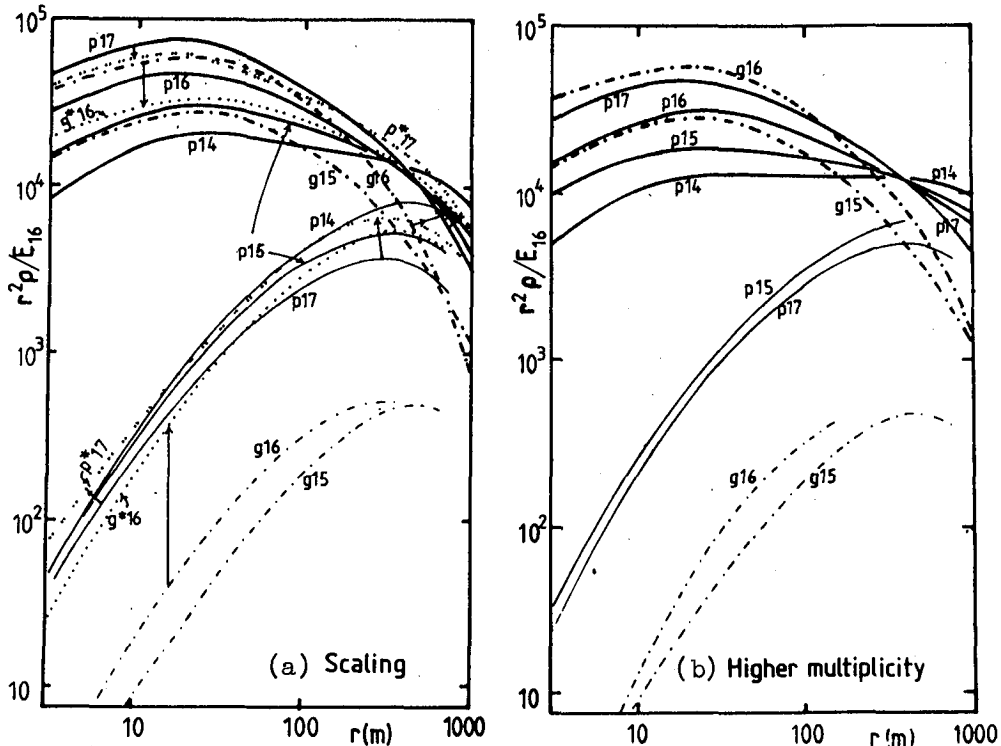


Figure 1: Particle densities (in water tank) and muon densities in proton and gamma-initiated showers at 15° to vertical (Sea level).

muon densities above 0.4 GeV (as at Haverah Park). Graphs 1(a) and 1(b) use the two different hadronic interaction models. Muon densities, in the lower part of the graphs, are shown by thinner lines. The gamma showers (---) differ from the proton showers by having a very much lower muon density — as expected from calculations by Wdowczyk long ago (2), and this helps to make the overall particle density fall more steeply beyond 200m — though this effect is less marked in scintillators.

As an alternative to muon detection may be to compare particle densities recorded by deep and shallow detectors, the ratio of (120 cm) water tank signal (ptcle. density) to (5 cm) scintillator density is plotted in Figure 2 for 10^{16} eV proton showers (line and dashed curve show results

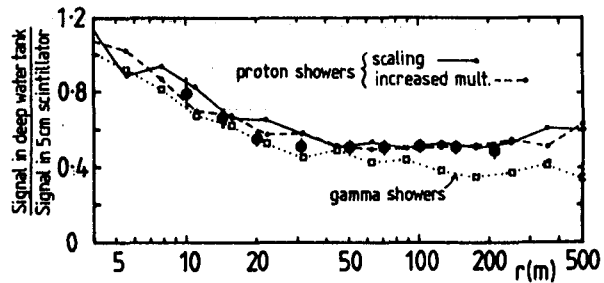
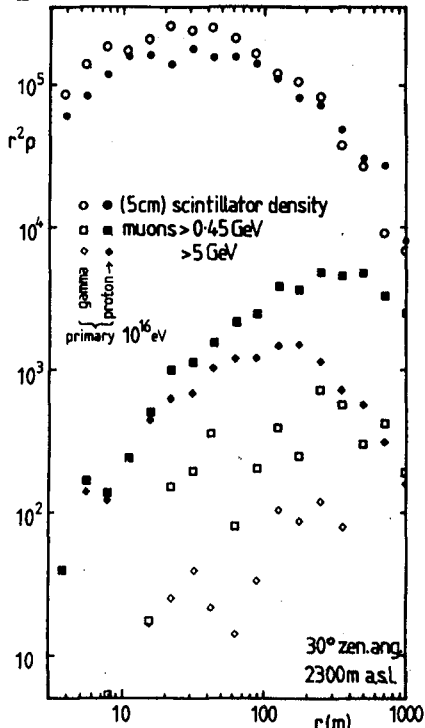


Figure 2 (\uparrow). Ratio of particle densities recorded by two detectors in proton and gamma showers at various axial distances. (Sea level: zenith angle 15° : energy 10^{16} eV or thereabouts.)

\leftarrow Figure 3. Predicted particle densities ρ in proton (filled symbols) and gamma showers (open symbols) of 10^{16} eV at high altitude site (2300 m). Showers at 30° zenith angle. Detectors are 5-cm scintillators.

from the two models) and gamma showers (dotted curve). Mean ratios in showers of $\sim 3 \times 10^{16}$ eV at $\sim 13^\circ$ zenith angle have been observed for ordinary real showers (filled circles: J. Perrett & A. A. Watson, private communication), and agree fairly well with expectation. (The sensitivity to the proportion of heavy nuclei is not calculated here, but is not a major factor in the present comparison.) Measurements are required beyond 100m with very large detector areas to make use of the expected peculiarities of individual gamma showers.

Figure 3 shows what is expected (from the scaling model) at a high level observing station (2300m altitude), looking at 10^{16} eV gamma showers and proton showers at 30° zenith angle (typical for Cygnus X-3). Scintillator particle densities are plotted. The statistical accuracy of this simulation run for gamma showers is too low to give a good determination of their muon densities, though the shape of the muon curve should be very similar to the curves in Figure 1.

4. Do gamma-rays produce hadrons much more frequently?

This would, of course, invalidate the previous graphs.

Figure 4 shows the density of muons above 2 GeV at 10m from the shower axis, interpolated from the calculations for protons (line p - both models agree here) and gammas (line g). A line for iron primaries (Fe) is also shown. The Kiel results (1) for nuclear and (presumed) gamma showers are marked. There is a huge discrepancy. So, do electrons or photons of high energy generate pions or muons readily by some unknown process? Would this not wreck all interpretations of air showers?

To begin an exploration of the latter question, a quite arbitrary large addition has been made to the hadronic cross-section for photons at

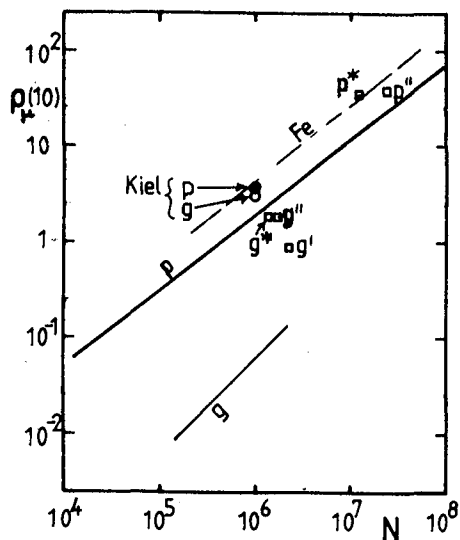


Figure 4. Densities of muons (>2 GeV) at 10 m from shower axis in nuclear (p, Fe) and gamma (g) showers.

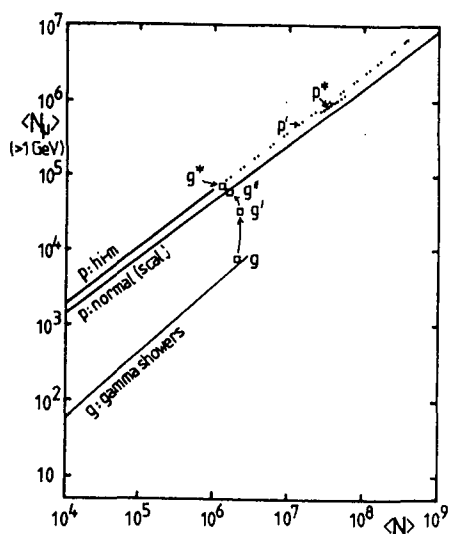


Figure 5. Number of muons (>1 GeV) & total shower size N . See text.

high energy (no change below 1 TeV) — either (i) a very broad resonance at a few TeV, the interaction m.f.p. at its peak being 100 g cm^{-2} (result: muon density in gamma showers shown as g') — or (ii) the same but with m.f.p. 40 g cm^{-2} at peak (g'' , and point p'' for 10^{17} eV proton EAS) — or (iii) cross-section having threshold above 1 TeV, and m.f.p. remaining at 100 g cm^{-2} above 10 TeV (g^* and, for proton showers, p^*). Clearly, gamma showers are now hardly distinguishable from proton showers by their muon content — and their lateral distributions become more similar. (See Fig. 1: the line shows the modified 10^{16} eV gamma showers, g^* , and the line shows the resulting change to the structure of ordinary 10^{17} eV proton showers. The latter are in fact a surprisingly good fit to observations!)

One would expect the N_{μ} - N_e relationship for showers to be spoiled — perhaps $N_{\mu} \propto N_e$ now? Figure 5 shows that this is not the case. (The mean N_{μ} ($E_{\mu} > 1 \text{ GeV}$) is plotted against total number of particles (N) in the shower. For the purpose of this simple test only the averages $\langle N \rangle$ for fixed E_{primary} are plotted, without applying the small correction for primary spectrum selection bias.) Such an (arbitrary) assumption about photon interactions would also be expected to ease the problem of accounting for the ratio of multi-TeV hadrons and gammas in the atmosphere.

The alternative of considering direct muon production, or production via charm rather than by pions, has not been explored. Pions have the advantage of putting their energy into many lower-energy muons, after cascading.

Such a large hadron-like cross-section has no theoretical justification: can it really be possible? It would perhaps not have been noticeable in emulsion calorimeters with short (Pb) radiation lengths.

References

1. Samorski, M. & Stamm, W. (1983) 18th Int. C. R. Conference, Bangalore, 11, 244-7.
2. Wdowczyk, J. (1965) 9th Int. Conf. on Cosmic Rays, London, 2, 691-3